Encapsulation of Lysozyme in a Biodegradable Polymer by Precipitation with a Vapor-over-Liquid Antisolvent

TIMOTHY J. YOUNG, KEITH P. JOHNSTON,* KENJI MISHIMA, AND HIROYUKI TANAKA

Contribution from *Department of Chemical Engineering, University of Texas, Austin, Texas 78712.*

Received May 31, 1998. Accepted for publication March 10, 1999.

Abstract □ Lysozyme was encapsulated in biodegradable polymer microspheres which were precipitated from an organic solution by spraying the solution into carbon dioxide. The polymer, either poly(*l*-lactide) (*l*-PLA) or poly(DL-lactide-*co*-glycolide) (PGLA), in dichloromethane solution with suspended lysozyme was sprayed into a CO_2 vapor phase through a capillary nozzle to form droplets which solidified after falling into a CO_2 liquid phase. By delaying precipitation in the vapor phase, the primary particles became sufficiently large, from 5 to 70 μm, such that they could encapsulate the lysozyme. At an optimal temperature of −20 °C, the polymer solution mixed rapidly with CO_2, and the precipitated primary particles were sufficiently hard such that agglomeration was markedly reduced compared with higher temperatures. More uniform particles were formed by flowing CO_2 at high velocity in a coaxial nozzle to mix the droplets at the CO_2 vapor–liquid interface. This process offers a means to produce encapsulated proteins in poly(DL-lactide-*co*-glycolide) microspheres without earlier limitations of massive polymer agglomeration and limited protein solubility in organic solvents.

Introduction

Microencapsulation of pharmaceutical compounds in biodegradable polymer particles is of great interest for controlled-release in oral, inhalation, or injection methods of delivery. Typical methods of microencapsulation include emulsion−solvent-extraction, spray-drying, and phase-separation techniques.[1−7] Potential drawbacks associated with these techniques include the use of toxic organic solvents for solubility, residual solvent in the microspheres, low encapsulation efficiencies due to partitioning of the pharmaceutical compound between two immiscible phases, and denaturation. The biodegradable homopolymers poly(*l*-lactic acid), poly(DL-lactic acid), poly(glycolic acid), and copolymers of these have been of particular interest as carrier substances.[8−13]

Several supercritical fluid processes have been utilized to form microparticles of polymers and pharmaceutical compounds. To manipulate particle morphology, the solvent power of compressed CO_2 can be changed by adjusting the temperature and pressure.[14,15] The critical conditions of CO_2 are easily attainable, i.e., T_c = 31 °C and P_c = 73.8 bar. This environmentally benign solvent is essentially nontoxic, nonflammable, and inexpensive. Phase separation techniques based upon supercritical fluids include rapid expansion from supercritical solution (RESS),[13,16−27] gas antisolvent recrystallization (GAS),[27−30] and precipitation with a compressed fluid antisolvent (PCA),[31−43] also known as aerosol solvent extraction system (ASES)[44−47] or supercritical antisolvent technique (SAS).[44] RESS is useful for materials which are soluble in CO_2. Unfortunately, CO_2, with no dipole moment and a very low polarizability, is a very weak solvent and dissolves very few polymers.[48,49] RESS of a highly soluble polymer, poly(1,1,2,2-tetrahydroperfluorodecyl acrylate),[24] from CO_2 produced submicron particles and fibers.

Recently, microparticles have been formed by precipitation with compressed CO_2 in the liquid and supercritical fluid states.[31−47] The PCA process consists of atomizing a solution into compressed liquid or supercritical fluid CO_2. The atomization process may be accomplished by spraying at high velocities through a small nozzle (typically 100 μm) or by sonication[43] through a larger nozzle. The organic solvent diffuses rapidly into the bulk CO_2 phase, while CO_2 diffuses into the droplets, thereby precipitating the polymer. The rate of diffusion in both directions and thus the degree of supersaturation are higher than in the case of conventional liquid antisolvents, often resulting in submicron to micron-sized particles. More viscous polymer solutions at higher polymer concentrations lead to fibers with micron-sized features.[33,37] Several studies have shown very low concentrations of residual solvent in the product materials, especially after a CO_2 extraction step upon completion of the spray.[29,50−52]

Microspheres may be formed for semicrystalline polymers such as poly(*l*-lactic acid) (*l*-PLA) without flocculation and agglomeration at 40 °C.[29,30,38,41,43,45,46] Amorphous polymers, on the other hand, such as polystyrene (PS),[32,39,41] poly(methyl methacrylate) (PMMA),[39] and poly(DL-lactide-*co*-glycolide) (PGLA)[38] often flocculate and agglomerate. The loss of individual particles is a result of plasticization of the polymer by CO_2, which can be further influenced by residual solvent in CO_2. CO_2 can depress the T_g of PMMA by 100 °C below the normal value of 105 °C.[39,53] Upon exposure of PS to CO_2, the temperature at which stationary particles agglomerate corresponds closely with the depressed T_g.[34] For PGLA, agglomeration was present from 0 to 23 °C.[38] Severe agglomeration can occur when poly(d,l-lactide) microspheres precipitate from toluene solution by addition of 2-propanol as the phase-separating agent.[54] However, at temperatures between −40 °C and −100 °C the microspheres become sufficiently firm to avoid agglomeration.

A novel variation of the PCA process was used to form hollow spheres (microballoons) of polystyrene from polystyrene in toluene solutions with concentrations above 6 wt %.[38] In this case the cell was filled only partially with liquid CO_2, with its equilibrium vapor phase above it. The solution was atomized in the vapor phase, and the droplets subsequently fell into the liquid phase where they solidified. By delaying precipitation in the vapor phase, hollow microspheres were formed. The microballoons were slightly larger than the diameter of the nozzle, and it is conceivable that they could be used to encapsulate a pharmaceutical compound.

A key challenge in the PCA process is to maintain the biological activity of proteins, peptides, and enzymes.[35] The dissolution of insulin, lysozyme, and trypsin into a typical solvent for PCA, like DMSO, denatures these proteins, probably due to a change in conformation.[55] Each of these materials remained denatured after processing via PCA. The bioactivity of certain proteins such as insulin and lysozyme recover upon redissolution into an aqueous

10.1021/js980237h CCC: $18.00
Published on Web 04/24/1999

environment, suggesting the interactions causing denaturation can be partially reversible.[44,56] A recent study also suggests that long-term storage of proteins which have been denatured by supercritical fluid processing, such as lysozyme, does not severely alter the stability and ability to recover bioactivity.[57]

The objective of this study was to encapsulate chicken egg-white lysozyme into uniform 50−100 μm poly(DL-lactide-*co*-glycolide) (PGLA) spheres. Smaller particles would be too small to encapsulate a significant number of 5−10 μm protein particles for controlled-release purposes. Larger particles would be undesirable for certain administration methods; for example, parenteral administration requires particles <100 μm in diameter.[58] The first part of this study examines the particle morphology for PGLA particles formed by PCA without any protein present. To produce larger primary particles than the 1−5 μm particles typically produced by PCA in liquid or supercritical CO_2,[31,32,35,36,38−42,44,45,59] we chose to delay precipitation by spraying into a CO_2 vapor phase above a CO_2 liquid phase. Another goal was to achieve high enough local concentrations of polymer in the droplets striking the CO_2 liquid phase to allow significant particle growth, while avoiding agglomeration. To attempt to minimize agglomeration caused by plasticization of the polymer by CO_2, the temperature was varied from 23 to −40 °C. The effects of nozzle diameter, solution flowrate, CO_2 flowrate, and solution concentration were also evaluated. In the second part, we address microencapsulation of chicken egg-white lysozyme into the polymer particles. Lysozyme was suspended in dichloromethane, in contrast with earlier studies where a protein was dissolved in an organic solvent.[27,30,38,43,46] Suspensions may be formed for a broad range of peptides and proteins, many of which are insoluble in organic solvents. Suspension of a protein in an organic solvent typically produces less denaturation than dissolution. The knowledge gained from the study of PGLA particle formation in the first part was utilized to encapsulate lysozyme in nonagglomerated particles with diameters in the 50−100 μm range as desired. In both parts of this study, separate sections are presented to delineate between experiments in static (nonflowing) and flowing CO_2.

Experimental Section

Materials—Semicrystalline poly(*l*-lactic acid) (*l*-PLA) (MEDISORBTM 100L, Stolle-Dupont Co. Cincinnati, OH) had a M_w of 94100 and a M_w/M_n of 1.85. Poly(DL-lactide-*co*-glycolide) (PGLA) was purchased from Birmingham Polymers, Inc. (Birmingham, AL) and had a M_w of 30000. Chicken egg-white lysozyme (Sigma, St. Louis, MO) was spray-dried from aqueous solution to form 1−10 μm particles. Ruthenium tetroxide (Electron Microscopy Sciences, Fort Washington, PA), reagent grade dichloromethane, and bone dry grade CO_2 were used as received.

Apparatus—The apparatus for precipitation with compressed CO_2, shown in Figure 1, is based upon earlier designs.[35,40] The solutions were sprayed into a 1.27 cm. i.d. sapphire tube with a volume of 13 mL. This tube allowed visual observation of skin formation in falling droplets, jet dynamics, and polymer precipitation. Visual observations proved invaluable in optimizing the PCA process. A thermostated water bath was utilized for experiments performed above 0 °C, while a dry ice−ethanol bath was used for subzero temperatures. For all experiments, the CO_2 level inside the cell was maintained 1 cm below the tip of the spray nozzle. The CO_2 inlet line (30 feet long, 0.030 in. i.d. by 1/16 in. o.d.) was immersed in the bath to equilibrate the CO_2 temperature prior to introduction into the cell.

A cylindrical tube (1 in. o.d. by 11/16 in. i.d. by 8 in. long, Autoclave Engineers, model CNLX 1608−316) rated up to 689 bar equipped with a piston was used to pressurize the polymer solution. This tube was pressurized with dichloromethane by using a computer-controlled syringe pump (ISCO, model 260D). The

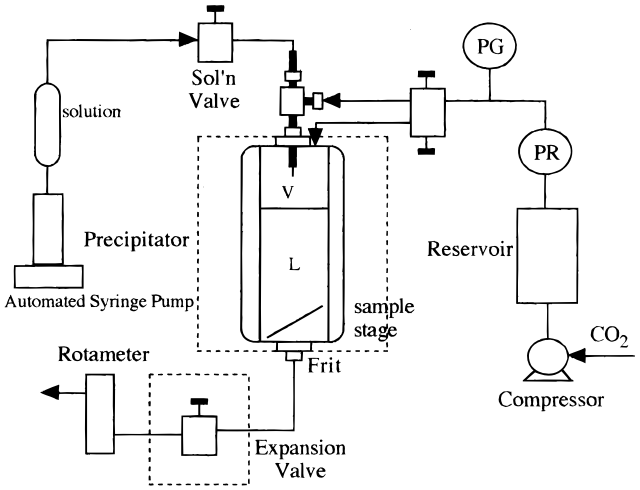

Figure 1—Schematic of the apparatus for precipitation with a vapor-over-liquid compressed fluid antisolvent.

polymer solution was sprayed into the cell via a 100 μm i.d. fused silica capillary tube or a 0.030 in. i.d. stainless steel tube. In all cases, the nozzle length was 6.5 in. Nozzles smaller than 100 μm could not be used because they were plugged by the suspended lysozyme particles. To ensure smoothness, the capillary tips were inspected with a microscope. The lysozyme was suspended in the polymer solution by using an ultrasonic bath.

To collect particles, two small rectangular glass plates (1 in. by 1/4 in.), slanted at an angle of 60°, were stacked in the bottom of the cell with approximately 5 mm between them. These glass plates were partially covered with double-sided carbon conductive tape. Also, a 1/4 in. diameter 0.5 μm filter was placed in the CO_2 effluent line at the base of the precipitation cell.

The solution flow rate was controlled with the automated syringe pump, and in most cases the solution was dripped into the cell at 0.1−1.0 mL/min. The solution was injected into a vapor CO_2 phase residing above a liquid CO_2 phase. In some cases, the solution flowrate was increased to ~1.8 mL/min where the solution no longer dripped, but instead streamed into the cell. This stream subsequently broke up into smaller droplets upon contacting the CO_2 liquid surface. For most cases, the CO_2 was not flowing. In experiments with flowing CO_2, the CO_2 entered the cell either through a port in the top of the cell or through an annular region in a coaxial nozzle, described in detail elsewhere.[41] The CO_2 flow rate was controlled by a needle valve (Whitey, SS-21RS4) in the effluent line and measured by a rotameter (Omega, model FLT-40ST). To prevent freezing due to CO_2 expansion, the valve was heated in a water bath to greater than 50 °C. Upon completion of solution injection, the cell was filled with liquid CO_2 to a pressure of 103 bar. Liquid CO_2 was swept through the cell for 10 min to remove the dichloromethane and further dry the particles. After drying, the cell depressurized over a 15 min span.

Characterization—Scanning electron microscopy (SEM) (JEOL JSM-35C) was used to analyze the morphology of the polymer particles. The glass slides were mounted on a SEM stage and coated to an approximate thickness of 200 Å (Pelco Model 3 Sputter Coater).

To detect lysozyme within the particles, two techniques were used. In the first method, the lysozyme was stained by ruthenium tetroxide prior to suspension in the polymer solution, and the product was observed with an optical microscope (Olympus VANOX-T or Olympus C-35AD-2)) and compared with SEM images of the same particles. Energy dispersive spectroscopy (EDS) was used as the second method (Kevex Analyst 8000 Microanalyzer). Two of the amino acids present in lysozyme, cysteine and methionine, contain sulfur, which is not present in the polymer, and can be detected by this technique.

Results and Discussion

Effect of CO_2−Dichloromethane Mixtures on Morphology of Polymers—For the CO_2 antisolvent process to be successful, the polymer must be highly insoluble in

Table 1—Morphology of Particles Produced by Dripping Homogeneous Solutions of Amorphous Poly(DL-lactide-*co*-glycolide) and Semicrystalline Poly(*l*-lactide) in Dichloromethane into Vapor-over-liquid Carbon Dioxide

polymer	C_{soln} (wt %)	temp (°C)	Q_{soln} (mL/min)	Q_{CO_2} (mL/min)	spray time (min)	particle size (μm)	comments
PGLA	1.0	–20	0.22	0.0	0.35	0.5–5	particles
	5.0	–20	0.22	0.0	0.17	5–70	particles
	5.0	1	0.10	0.0	1.37	10–50	some 500 μm agglomerates
	5.0	5	0.10	0.0	0.35	5–15	some 500 μm agglomerates
	10.0	–20	4.0	0.0	0.33	—	1000 μm agglomerates
	1.0	–30	0.21	0.0	0.36	—	1000 μm agglomerates
	5.0[a]	–20	0.13	0.0	4.66	—	1000 μm agglomerates
	5.0[b]	–18	0.5	17.5	1.68	3–25	particles
	5.0[b,c]	0	0.5	35	0.35	10–50	some 500 μm agglomerates
l-PLA	1.0	20	0.5	0.0	0.45	1–4	particles
	5.0[c]	24	0.5	0.0	0.58	250–500	particles

[a] 750 μm i.d. nozzle. [b] CO_2 flow through coaxial nozzle. [c] 0.5 wt % lysozyme also present.

the CO_2–organic solvent mixture, and this mixture must not cause too much agglomeration of the polymer. Previously, it was shown that lower molecular weight *l*-PLA is only slightly soluble in CO_2–cosolvent mixtures.[18] CO_2 does not cause *l*-PLA particles to agglomerate, since they are semicrystalline.[38] *l*-PLA has a melting temperature (T_m) of 173–178 °C and a glass transition temperature (T_g) of 60–65 °C (manufacturer's data). The amorphous biodegradable polymer poly(DL-lactide-*co*-glycolide) (PGLA), however, is highly plasticized by CO_2. PGLA has a T_g of 45–50 °C.

Experiments were performed to determine if CO_2 causes PGLA particles to agglomerate. PGLA, as a powder, and in some cases dichloromethane, as a liquid, were fed into a high-pressure cell equipped with a sapphire window which has been described previously.[60] The cell was sealed, and then liquid CO_2 was injected slowly into the cell. From ambient temperature down to 0 °C, PGLA powder quickly gels into a viscous mass when in the presence of liquid CO_2 for concentrations from 0.01 to 1.0 wt %. At these concentrations, very little polymer dissolved, even with up to 5 wt % CH_2Cl_2 as a potential cosolvent. The cosolvent concentrations were chosen to mimic conditions used in the PCA process. Upon depressurization, the polymer foamed. At −20 °C, the polymer powder occasionally stuck to the wall of the cell, but was also partially suspended throughout the cell. At temperatures below −40 °C the polymer remained as a free-flowing, nonsticky powder. Since CO_2 acts as a plasticizer, it can lower the T_g of the polymer. The T_g of PGLA containing dissolved CO_2 could easily be as low as −40 °C, or even lower, based upon other systems mentioned previously.[34,39,53,54]

Organic Solvent–CO_2 Miscibility and Mixing—Dichloromethane is highly miscible with CO_2 at ambient temperature and pressures above 61 bar. In our investigations, concentrations as high as 73 wt % CH_2Cl_2 were miscible with liquid CO_2 at temperatures from 23 °C down to −46 °C. The mixing behavior of CH_2Cl_2 and CO_2 was observed inside the sapphire cell. The cell was filled partially with liquid CO_2 and equilibrated at the desired temperature and pressure. Pure dichloromethane was then injected into the cell through the 100 μm i.d. capillary nozzle. For conditions where the cell was only partially filled with liquid CO_2, i.e., vapor and liquid CO_2 phases were both present, the solvent was injected at flow rates of 0.5 mL/min or slower. This flow rate range prevented the solvent stream from atomizing and allowed the solvent to drip into the liquid phase. At temperatures ranging from ambient to −20 °C, the drops quickly dispersed into the liquid CO_2 phase upon contact. At colder temperatures (−30 °C and below) however, the drops were seen to fall about 1 cm through the liquid CO_2 phase before breaking up. Operating at temperatures at or below −30 °C therefore may be expected to delay precipitation of the polymer and/or lead to agglomeration due to insufficient mixing between the drop and liquid phases. While the solvent is still miscible with CO_2 at low temperatures, the rate of mixing decreases significantly.

Polymer Particles Formed in Static Vapor-over-Liquid CO_2—As shown in Table 1, the concentration of the polymer solution, temperature, solution flow rate, and CO_2 flow rate were manipulated to observe the effect on particle formation. In this section, the CO_2 was static (nonflowing). Since both a vapor and a liquid phase are present in each experiment, the initial pressure was simply the vapor pressure of CO_2 at a given temperature. At 0 °C the pressure was 35 bar, and at −20 °C it was 20 bar. As the solution was injected, the pressure decreased slightly, corresponding to the pressure of the CO_2/CH_2Cl_2 mixture. The liquid CO_2 level was maintained at 1 cm below the tip of the nozzle to allow droplet formation and release from the tip before contact with the liquid phase. With the low flow rate and low shear through the vapor phase, ~200 μm drops were formed at a frequency of approximately one per second.

l-PLA is a semicrystalline polymer which has been used many times in PCA to form microparticles without agglomeration.[13,29,38,41,43,45,46] Therefore, we first present results for *l*-PLA to serve as a basis for understanding the more challenging experiments with amorphous PGLA. When a 1.0% solution of *l*-PLA in dichloromethane was dripped into vapor-over-liquid CO_2 at 0.5 mL/min and 20 °C, the result was microspheres 1–4 μm in diameter, as shown in Figure 2 (top) and Table 2. On the basis of visual observation, it appeared that little precipitation occurred before each droplet contacted the liquid phase. After the droplet fell into the liquid CO_2 phase, rapid mass transfer led to intense nucleation resulting in the small microspheres. This result indicates atomization does not play as important a role in achieving small particles as suggested previously.[41] The particles formed a free-flowing powder and could be sprayed for several minutes with no agglomeration even as solvent accumulated inside the cell.

Figure 3 is a schematic of a ternary phase diagram consisting of a polymer, organic solvent, and compressed CO_2.[32] The mass transfer pathways are shown only for the lower liquid CO_2 phase. Two of the binary systems are completely miscible at most conditions in this study, but the polymer–CO_2 binary system is only slightly miscible. The binodal (coexistence) curve separates the one-phase and two-phase regions in the ternary system. Between the binodal and spinodal curves is the metastable region. The system is stable to small concentration fluctuations in this region, and phase separation will be by nucleation and growth. Upon crossing the binodal curve for dilute polymer

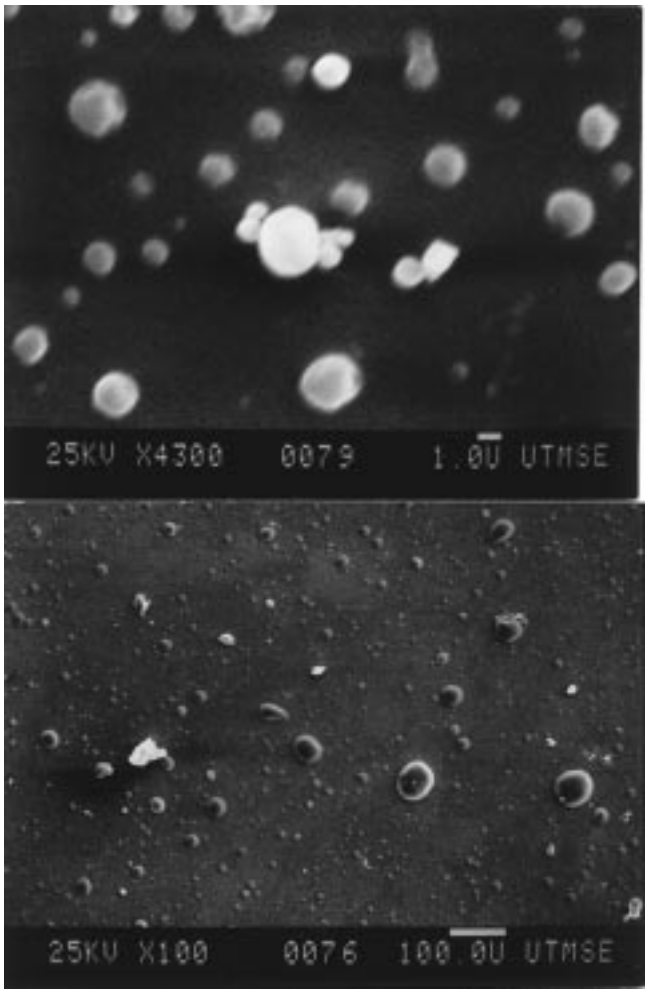

Figure 2—SEM micrographs of *l*-PLA microspheres (top) formed by spraying a 1.0 wt % *l*-PLA in dichloromethane (CH_2Cl_2) solution at 0.5 mL/min at 20 °C and PGLA microspheres (bottom) formed by spraying a 5.0 wt % PGLA in CH_2Cl_2 solution at 0.22 mL/min (T = –20 °C), both through a 100 μm capillary nozzle into static CO_2.

solutions, a polymer-rich phase will nucleate and grow within a solvent-rich continuous phase.

For a 5.0% solution of *l*-PLA sprayed at similar conditions, we observed skin formation on the backlit droplet while it was in the vapor-phase, and the resulting particles were 250−500 μm in diameter. It was easy to observe that the liquid droplet became opaque as it fell through the CO_2 vapor. A viscous skin appeared to form on the surface of the drop, and the drop did not break up upon contact with the liquid CO_2. This observation of skin formation is entirely consistent with SEM micrographs, which indicated that the particles were the same size as the droplets. In other experiments, at lower concentrations, where a skin did not form, a clear transparent droplet fell through the vapor. With the higher polymer concentration, the dissolution of CO_2 into the droplet forms a skin on the droplet while it is still in the vapor phase. At this concentration for *l*-PLA, the mass transfer pathway on the phase diagram in Figure 3 passes above the critical point on the binodal curve (curve B), thus a solvent-rich phase nucleates and grows within a polymer-rich phase causing skin formation. The polymer entanglement and viscosity in the skin are sufficient to maintain the integrity of the droplet as it solidifies in the liquid CO_2, as was observed in a similar system, as shown in Figures 4−10 of ref 34.[34] Here, the final particle size produced in each droplet is larger than the nozzle diameter, 100 μm, which was also the case for PS in toluene solutions sprayed into vapor-over-liquid CO_2.[34]

In vapor-over-liquid PCA when drops fall through vapor and atomization is not present, mass transfer is still fast enough in dilute solutions and is fast enough to produce 1−4 μm *l*-PLA particles, apparently following mass transfer pathway A in Figure 3. However, in a previous study with intense atomization into liquid CO_2 at a high density of 0.96 g/mL, the primary particle sizes were even smaller, from 0.1 to 1 μm.[41] Not only was atomization more intense producing smaller droplets, but the phase boundary was reached more quickly from the faster mass transfer. In addition, the polymer solidified more rapidly leading to smaller particles. Dilute solutions were not studied in the past for V/L CO_2, as, for example, the concentration was 6 wt % or higher for PS solutions and particles were larger than 100 μm.[34]

For PGLA, the solution concentration was varied from 1.0 to 10.0 wt %. To prevent agglomeration, most experiments were performed at −20 °C to raise the polymer solution viscosity sufficiently, while maintaining high enough rates of CO_2−organic solvent mixing (on the basis of the above visual observations of mixing). Also, spray times were generally kept short, <30 s, to avoid accumulating large concentrations of dichloromethane in the static CO_2, which causes agglomeration. As the polymer concentration and thus the solution viscosity increased, it became necessary to raise the solution flow rate to maintain a constant droplet size. The size was chosen to be slightly larger than the nozzle's inner diameter. At 1.0 wt % and −20 °C, small 0.5−5 μm particles were formed by dripping the solution at a flow rate of 0.22 mL/min into CO_2. These nonagglomerated particles were similar to the *l*-PLA microspheres shown in Figure 2 (top). The same experiment conducted at 0 °C and above produced some small (0.5−5 μm) primary particles but mostly large (>500 μm) solid agglomerates. Therefore, the polymer particles are significantly more viscous and less susceptible to agglomeration at −20 °C.

As shown in Figure 2 (bottom), a 5.0 wt % solution resulted in 5−70 μm microspheres. At this higher concentration, larger particles may be expected because of the higher solution viscosity. When the large droplet strikes the liquid surface, the more viscous solution mixes more slowly with the surrounding liquid CO_2 and mass transfer rates are slower. With slower mixing and mass transfer, the degree of supersaturation is lower than with less viscous solutions (lower concentrations), resulting in fewer nuclei per weight of polymer. Because most of the nuclei tend to be formed in a small volume where the droplet falls, coalescence of primary particles is more prevalent than for the experiments with lower polymer concentrations, where faster mixing occurs. With the reduction in nucleation rate and higher polymer concentrations (which produces faster agglomeration), especially in a local volume where the drop falls, larger particles are formed.

Unlike previous studies for polystyrene with the same vapor-over-liquid technique, these particles are much smaller than the initial droplet size, which was ~200 μm. For 6 wt % polystyrene (200000 MW) in toluene solutions, 300 μm diameter microballoons are formed with a 151 μm nozzle.[34] A skin, about 20 μm thick, forms on the droplet while still in the vapor phase which then hardens upon contact with the liquid phase. The polymer entanglement and viscosity in the skin are sufficient to maintain the integrity of the droplet as it solidifies in the liquid CO_2. The PGLA in this study has a much lower molecular weight (~30000), and the solutions are much less viscous. Also, the miscible region in the phase diagram in Figure 3 is

Table 2—Morphology of Particles Produced by Dripping Homogeneous Solutions of Amorphous Poly(DL-lactide-*co*-glycolide) and Semicrystalline Poly(*l*-lactide) in Dichloromethane Containing Suspended Lysozyme into Vapor-over-Liquid Carbon Dioxide

polymer	C_{soln} (wt %)	temp (°C)	Q_{soln} (mL/min)	Q_{CO_2} (mL/min)	spray time (min)	particle size (μm)	encapsulation
PGLA/lysozyme	1.0 /0.1[a]	–23	0.1	0.0	0.48	0.5–5	no
	5.0/0.5	–20	0.1	0.0	1.28	10–60	yes
	5.0/0.5	–20	0.5	0.0	0.63	10–50	yes
	5.0/0.5	–20	1.5	0.0	0.28	5–50	yes
	5.0 /0.5[b]	–20	1.8	0.0	0.18	5–60	yes
	5.0 /0.5[c]	–20	0.5	25	0.42	5–30	yes
	5.0 /0.5[d]	–21	0.5	35	0.82	>1000[e]	no
l-PLA/lysozyme	1.0/0.1	20	0.1	0.0	3.23	0.5–2.5	no
	5.0/0.5	24	0.5	0.0	0.58	250–500	yes

[a] 1.0 wt % PGLA, 0.1 wt % lysozyme. [b] Onset of streaming due to high Q_{soln}. [c] CO_2 flow through coaxial nozzle. [d] CO_2 flow enters from top of cell. [e] Agglomerates.

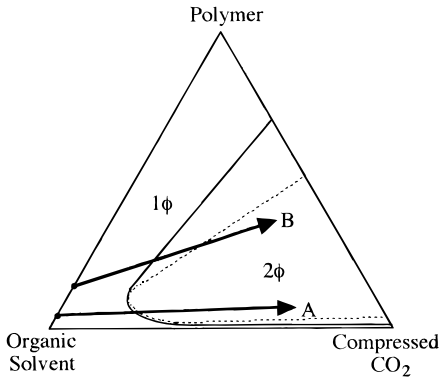

Figure 3—Schematic ternary phase diagram comparing mass transfer pathways for precipitation with a compressed fluid antisolvent: (—) binodal curve, (---) spinodal curve.

larger for PGLA–dichloromethane–CO_2 than for PS–toluene–CO_2 because of the lower molecular weight for PGLA versus PS and the lower solubility parameter of dichloromethane versus toluene. Consequently, it will take longer for PGLA to precipitate on the mass transfer pathway on the phase diagram (Figure 3), delaying skin formation.[34] Without any visual indication of skin formation in the vapor phase, smaller particles are produced, as the droplet breaks up on contact with the liquid phase.

At dilute concentrations, PGLA does not appear to form a skin when contacting CO_2 vapor, and the particles do not form until the large droplet has begun to disperse in the liquid CO_2 phase. When the solution concentration is increased to 10 wt %, the solution becomes extremely viscous and individual particles are not formed, only large agglomerates, >1000 μm. Here, a thin skin is visible on the droplets while they are being formed in the vapor phase, although the microscopic structure of the skin could not observed with the naked eye. The formation of a skin was confirmed by examination of the samples with SEM (not shown). Skin formation is favored by the higher solution viscosity and high concentration, which may shift the mass transfer pathway above the critical point (see Figure 3). This shift would cause solvent-rich domains to nucleate and grow within a polymer-rich domain.[34,37] The thin skin is weak, since it contains a high concentration of dissolved CO_2, and it was easy to observe visually that the skin immediately ruptures upon hitting the CO_2 liquid surface. The ruptured skin appeared as large agglomerates or films when examined by SEM (not shown). The mixing and diffusion of solvent away from the droplet are very slow due to the high polymer concentration and viscosity, resulting in severe agglomeration.

When a polymer solution is sprayed at 1.0 mL/min into flowing liquid CO_2 (without a CO_2 vapor phase), we found that fibers are produced for PGLA concentrations above 1.0 wt %. Fibers are formed from the jet due to the rapid nucleation, high solution concentration, high solution viscosity (to prevent atomization) and skin formation.[33] In experiments with vapor-over-liquid CO_2, the large droplets are formed instead of a jet (at the same flow rate) due to much higher interfacial tension because of the low CO_2 density. The precipitation in the droplets is slower than in the case of a jet due to the larger dimensions of the solution phase and lower miscibility between the phases for CO_2 vapor compared with CO_2 liquid. As a result, fibers are not formed.

The opposing effects of temperature on particle growth, coalescence, and mixing between the phases must be properly balanced to produce large nonagglomerated particles. As temperature is decreased the polymer solution becomes more viscous, which will cause coalescence to be less prevalent. Some coalescence, however, will aid the formation of the desired 50–100 μm particles rather than the typical 1–5 μm particles. As mentioned earlier, decreasing the temperature below −20 °C slows the mixing between the solvent and CO_2 phases. When a 1.0% solution of PGLA in dichloromethane was dripped into liquid CO_2 at −30 °C, no distinct particles were formed, only large agglomerates, due to the slow mixing. When the solution droplets fell, they initially formed a pool at the liquid surface and then penetrated the surface. The polymer began to precipitate at the interface, forming a film, and occasionally droplets fell through the film and agglomerated. Previously, we showed that PGLA particles exposed to CO_2 do not tend to agglomerate at −40 °C, indicating hard particles or even a glassy state. Unfortunately, the rate of mixing between the organic solvent and the liquid CO_2 is too slow at −30 °C and −40 °C to disperse the polymer.

At temperatures higher than 0 °C, agglomeration also occurred readily. As seen in Figure 4 (top), a 5.0 wt % solution dripped into liquid CO_2 at 1 °C yielded some distinct particles in the 10–50 μm range, but the polymer was partially agglomerated. This occurred for every experiment at 0 °C or above since the polymer is excessively swollen by CO_2 and the viscosity is too low at these temperatures.

A 0.030 in. i.d. (~750 μm) stainless steel nozzle was used to form larger initial droplets in order to attempt to produce the desired particle size. For PGLA concentrations of 1.0 and 5.0 wt %, and temperatures from −20 °C to 4 °C, the particles were always severely agglomerated with few, if any, distinct particles. The large drops formed more slowly, providing more time for precipitation to occur which allowed a thin skin to form on the large droplets while in the vapor phase. On the basis of visual observation, this skin was weak and ruptured upon impact with the liquid

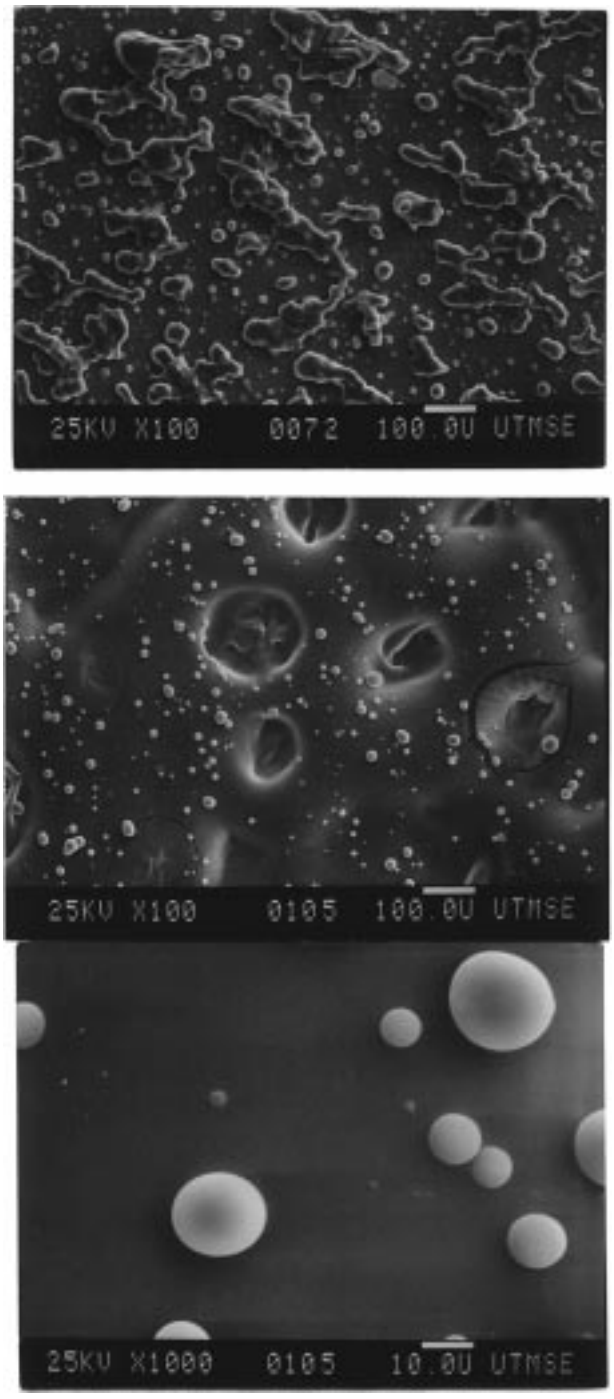

Figure 4—SEM micrographs of PGLA microspheres formed by spraying a 5.0 wt % PGLA in CH_2Cl_2 solution at 0.1 mL/min ($T = 1$ °C) into static CO_2 (top) and at 0.5 mL/min into CO_2 flowing at 17.5 mL/min at –20 °C (middle and bottom) through a 100 μm capillary.

CO_2 surface. The larger droplet size produced a larger local concentration of polymer and solvent which caused severe agglomeration of the polymer.

Polymer Particles Formed in Flowing Vapor-over-Liquid CO_2—Experiments were performed with flowing CO_2 to minimize CH_2Cl_2 accumulation. CO_2 was passed through the annular region of a coaxial nozzle, described previously,[41] at high velocity (69−138 cm/s) to agitate the surface of the liquid phase to enhance mixing. Figure 4 (middle and bottom) shows PGLA particles formed by spraying a 5.0 wt % solution at 0.5 mL/min into the cell through a 100 μm capillary nozzle with CO_2 flowing at 17.5 mL/min and at −20 °C. Vigorous mixing was observed at

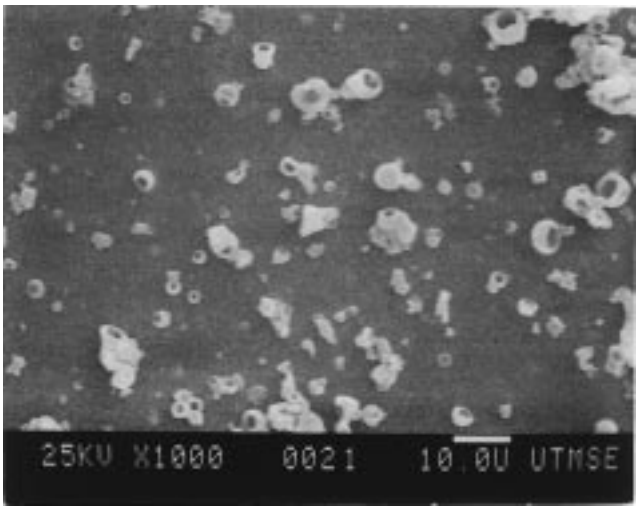

Figure 5—SEM micrograph of spray-dried lysozyme particles.

the interface, such that particles nucleated and grew throughout the liquid-phase rather than in a local region where the droplets fell. The resulting spherical particles ranged in size from 3 to 25 μm in diameter with no agglomeration even after almost 2 min of spraying. The difference in results was dramatic compared to the case for static CO_2. The particles were suspended throughout the cell, but plugging of the frit in the effluent line at the bottom of the cell limited spray times. This problem could be reduced in the future with a larger filter. The increased mixing causes a higher degree of supersaturation, more nucleation, faster solvent removal and quenching, and less time for growth. The result was far less coalescence and agglomeration when compared to the case with static CO_2. Experiments were also run at higher temperatures to determine if the increased mixing was enough to prevent agglomeration. For all cases where the temperature was 0 °C or higher, some 10−50 μm particles were formed, but mostly large (>500 μm) agglomerates were formed. The particles were not sufficiently hard at the higher temperatures to prevent coalescence.

Encapsulation of Lysozyme into PGLA with Static CO_2—In control experiments, lysozyme suspensions in CH_2Cl_2 were sprayed into CO_2 through a 100 μm capillary nozzle at temperatures from 23 to 0 °C. The lysozyme suspensions were formed with an ultrasonic bath and were stable for hours. The suspension flowed smoothly through the capillary, and the particle size (1−10 μm) and morphology of the product were identical to those of the original lysozyme, which is shown in Figure 5. The original spray-dried lysozyme particles and those removed after spraying into CO_2 were "bowl-shaped" when examined by SEM. Since the polymer particles discussed previously were spheres, it is easy to distinguish between polymer and protein particles.

Table 2 summarizes results of encapsulating lysozyme into PGLA. Again, the temperature was chosen as −20 °C to strike a balance between mixing favored at high temperatures and formation of hard, nonsticky particles in CO_2 which is favored at low temperatures. An initial loading of 10:1 by weight of polymer to protein was maintained in each case. Figure 6 (top) shows the result of spraying a 1.0 wt % solution of PGLA with lysozyme into static CO_2. The primary particle size was 0.5−5 μm in diameter with very little encapsulation of the similarly sized protein particles. The solution was too dilute for polymer particles to encapsulate a significant fraction of the protein particles. This result was anticipated, since it was shown above that small 0.5−5 μm PGLA particles are formed by precipitation

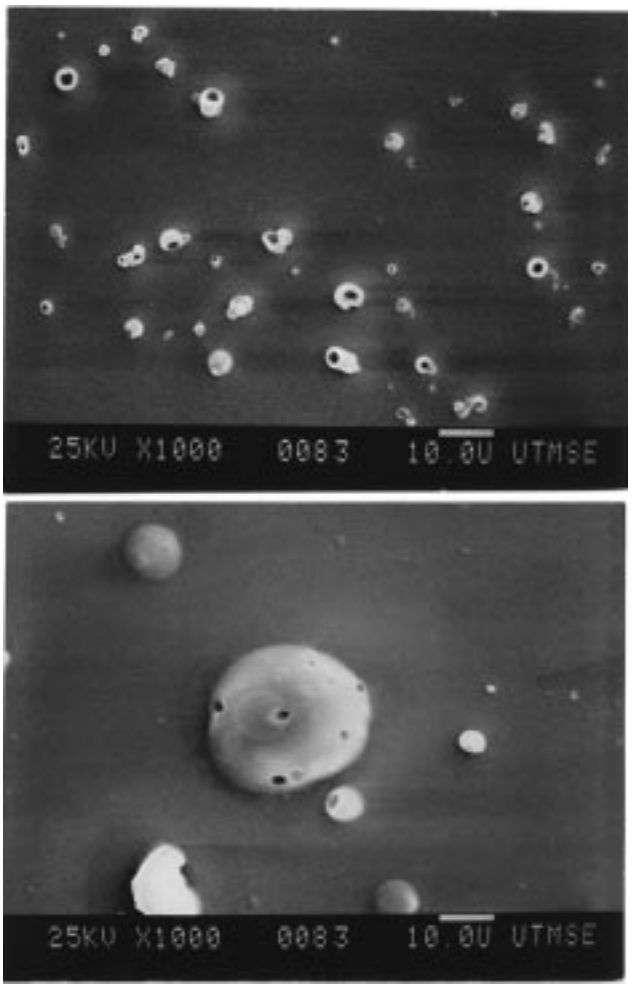

Figure 6—SEM micrographs of PGLA microspheres formed by spraying a 1.0/0.1 wt % (top) and a 5.0/0.5 wt % (bottom) PGLA/lysozyme suspension at 0.1 mL/min in CH_2Cl_2 through a 100 μm capillary nozzle into static CO_2 at –20 °C.

from a 1.0 wt % solution, which are too small to coat the lysozyme particles.

For a PGLA concentration of 5.0 wt %, the particles are in the 5−60 μm diameter range, and the encapsulation efficiency is substantial, as demonstrated in Figure 6 (bottom). Here, the magnification is high enough to examine a single particle. The craters or holes in the polymer particle represent protein particles for the following reasons. In identical experiments without protein, the craters were never present. Also, the size of the craters match those of the pure protein particles. Further evidence that the craters represent protein particles is given below in the subsection on experiments with flowing CO_2.

At lower magnifications, the particles looked similar to those shown in Figure 2 (bottom). Apparently, the presence of the small encapsulated protein particles does not have a significant influence on the polymer particle size. The polymer particles are much larger than in the case of a 1.0 wt % solution and are large enough to encapsulate multiple protein particles. Also, since the solution is more concentrated, the probability of a polymer particle nucleating and growing next to a lysozyme particle is enhanced. Also, the protein has the potential to act as a nucleating agent for the polymer. The large droplets formed in the CO_2 vapor phase lead to relatively slow mixing when the droplets strike the liquid CO_2 phase. The high local concentrations of the sticky CO_2-swollen polymer and protein lead to a large amount of growth.

A desirable feature of this spray geometry is that a polymer-rich phase nucleates in the presence of the protein in the confined space of the droplets, which occupy a small volume fraction compared to the total volume. Such nucleation may be expected to produce higher encapsulation efficiencies than if the polymer nucleated throughout the total cell volume. This advantage of compartmentalization of polymer and protein is not present in the GAS process cited above where CO_2 is added to a liquid solution. A disadvantage of the V/L PCA process is that the primary mass transfer takes place at the vapor−liquid surface rather than throughout the entire volume, which can lower the production rate.

Varying the size of the droplets leaving the nozzle could potentially lead to a change in size of the polymer particles. As the flow rate of the polymer solution increased, it was observed that the droplet size decreased. However, no significant change in particle morphology occurred when the solution flow rate was increased from 0.1 to 1.5 mL/min for a 5.0 wt % solution at −20 °C. In each case, the particles appeared as those shown in Figure 6 (bottom). A complication of extremely slow flow rates is plugging of the nozzle, which occurred very often at 0.1 mL/min, but infrequently at 0.5 mL/min or higher. This plugging is likely a result of precipitation inside the nozzle, caused by CO_2 diffusing upward into the nozzle and/or entrapment of the solid protein particles.

The degree of agglomeration of the polymer product is dependent upon the solution flow rate and spray time. When conducting the spray, at a certain time large particles could easily be seen with the naked eye. When analyzed by SEM, these large particles were agglomerates and not simply large flocculates of small primary particles. At a solution flow rate of only 0.1 mL/min, the experiment could be run for 1 min before agglomeration began to occur. For higher flow rates, the observed time where large particles appeared decreased accordingly to 40 and 20 s at flow rates of 0.5 and 1.5 mL/min, respectively. This agglomeration could potentially be avoided by either flowing CO_2 continuously through the cell as described in the next section or by spraying into a larger volume cell. At 1.8 mL/min, streaming of the solution begins to occur rather than dripping. Here, the range of particle sizes did not change, but there was a higher percentage of large particles compared to the previous cases at lower flow rates. Due to the large amount of solution flowing into the cell, agglomeration began to occur after only 10 s.

Encapsulation of Lysozyme into PGLA with Flowing CO_2—Figure 7 compares an optical micrograph and a SEM micrograph of polymer particles with protein particles visible on the surface. These particles were formed by spraying a 5.0 wt % PGLA solution with suspended lysozyme at 0.5 mL/min along with CO_2 flowing in the annulus at a velocity of 138 cm/s. The SEM image (top) shows particles with craters or holes in their surfaces, which may be identified as the "bowl"-shaped spray-dried lysozyme particles. The micrograph taken with the optical microscope (bottom) shows the same polymer particle with encapsulated stained protein particles. The stained protein directly corresponds to the craters observed in the SEM micrograph. This correspondence between optical and SEM photomicrographs was always observed where we compared images of particles formed by the vapor/liquid PCA process. Figure 8 (top) shows 40−70 μm particles with encapsulated lysozyme formed at the same conditions as Figure 7, except at a higher CO_2 flow rate. By varying the focal plane throughout the depth of the particle (not shown), we observed in the optical microscope that the protein particles were encapsulated throughout the PGLA particles and were not just on the surface. While there did

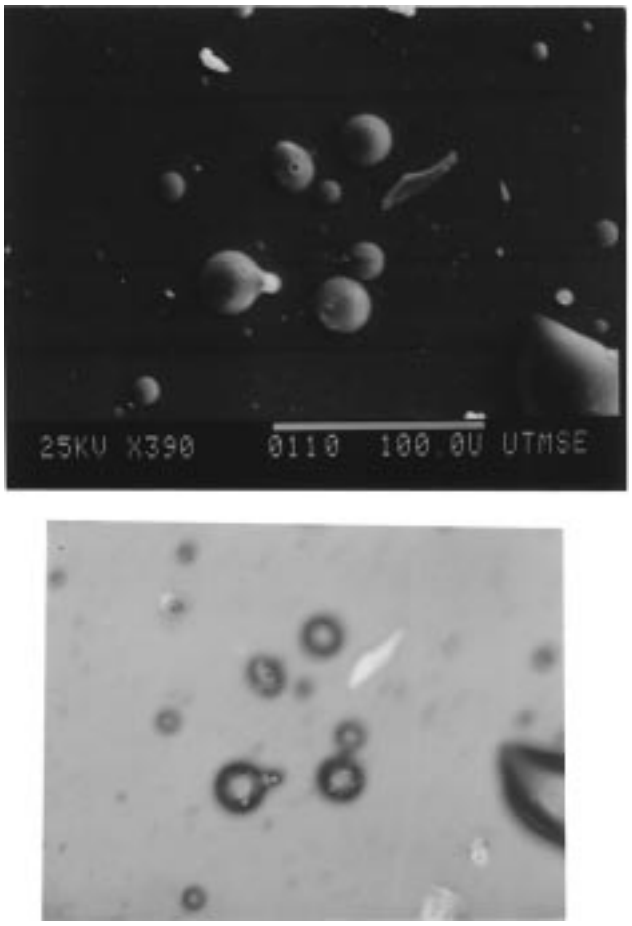

Figure 7—SEM micrograph (top) and optical micrograph (bottom) of PGLA microspheres formed by spraying a 5.0/0.5 wt % suspension of PGLA/lysozyme in CH_2Cl_2 at 0.5 mL/min through a 100 μm capillary nozzle into CO_2 flowing at 15 mL/min at –20 °C.

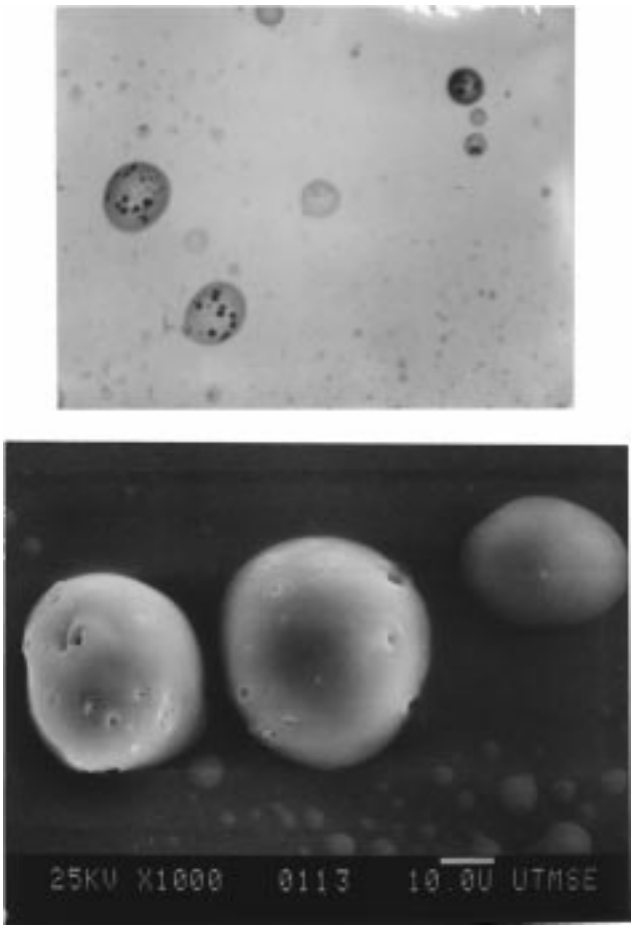

Figure 8—SEM micrograph (bottom) and optical micrograph (top) of PGLA microspheres formed by spraying at 0.5 mL/min a 5.0/0.5 wt %PGLA/lysozyme suspension in CH_2Cl_2 through a 100 μm capillary nozzle into CO_2 flowing at 25 mL/min at –20 °C.

not appear to be any protein particles which were not encapsulated, polymer particles without encapsulated protein were present.

Flowing CO_2 at high velocity during the spray delayed the time at which large particles were observed visually in the tube. This time corresponded to the time where agglomeration was observed in the SEM micrographs. Flowing CO_2 through the annular region surrounding the nozzle at high velocity caused a large amount of mixing at the vapor/liquid interface and suspended the precipitated particles throughout the cell, yielding spherical, nonagglomerated particles. Spraying a 5.0%/0.5% PGLA/lysozyme solution at 0.5 mL/min into the cell at −20 °C with CO_2 flowing at 25 mL/min yielded spherical particles 5−30 μm in diameter, with encapsulation of the protein as seen in Figure 8 (bottom). These particles are more uniform in size and shape than those formed in static CO_2 and appear like those in Figure 4 (middle). The particle sizes are more uniform in this case due to better mixing at the vapor−liquid interface.

In another type of experiment, CO_2 was introduced into the cell through a large opening located in the top of the cell 1 cm above the tip of the nozzle. Here, the CO_2 velocity was relatively low and turbulence from the CO_2 did not have much effect on the solution stream nor on the CO_2 vapor/liquid interface. The purpose of flowing CO_2 was to reduce the accumulation of solvent in the cell. Spraying a 5.0%/0.5% PGLA/lysozyme solution at 0.5 mL/min into CO_2 flowing at 35 mL/min at −21 °C yielded little change in particles size and failed to delay the onset of agglomeration, compared to the case with static CO_2. The same was true for higher CO_2 flow rates up to 52 mL/min. With this cell configuration, the CO_2 stream does not cause significant turbulence or mixing inside the cell. Since agglomeration occurred at the same time as in static CO_2 experiments, most of the agglomeration occurs immediately after precipitation and not after solvent buildup in the cell. In this case the particles were concentrated at the liquid−vapor interface and were not suspended throughout the liquid phase.

Elemental analysis via energy dispersive spectroscopy (EDS) was also used to confirm the presence of lysozyme in the polymer particles. Lysozyme has 2 amino acid constituents containing sulfur, cysteine, and methionine, which can be detected via EDS. Chicken egg white lysozyme is reported to contain eight cysteine molecules and two methionine molecules per protein chain.[61,62] Both of these amino acids have one sulfur atom per molecule, resulting in 10 per lysozyme molecule. EDS scans of the pure protein (top) and particles with encapsulated protein (bottom) are shown in Figure 9. The analysis of the pure lysozyme shows peaks corresponding to the presence of phosphorus, chlorine, and potassium impurities as well as the sulfur. Analysis of the peaks is only qualitative, unfortunately, due to multiple scattering of the X-rays. Particles formed by spraying a 5.0% PGLA solution with suspended lysozyme were analyzed as shown in Figure 9 (bottom). The lower curve represents a polymer particle with no protein present, while the upper curve corresponds to a single polymer particle with entrapped lysozyme. The particles were collected on a section of a glass slide, thus explaining the presence of the silicon impurity peak. The presence of the

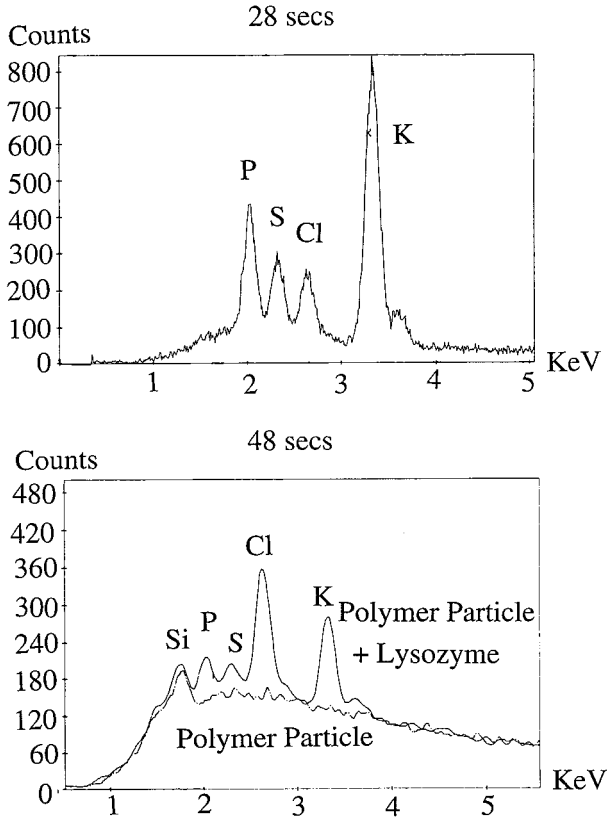

Figure 9—EDS scans of spray-dried lysozyme (top) and PGLA microspheres (bottom) formed by spraying a 5.0/0.5 wt % suspension of PGLA/lysozyme at 0.5 mL/min in CH_2Cl_2 through a 100 μm capillary nozzle into CO_2 flowing at 15 mL/min at –20 °C.

other peaks, excluding silicon, indicates that lysozyme was encapsulated within the polymer particle examined.

Encapsulation of Lysozyme into *l*-PLA—When polymer particles are similar in size to the protein particles, little or no encapsulation is expected to occur. Figure 10 (top) shows particles formed by spraying a 1.0% *l*-PLA solution with suspended lysozyme at 0.1 mL/min and 20 °C. As shown, the 1−4 μm polymer particles do not tend to encapsulate the lysozyme particles. Therefore, the polymer precipitation occurs without requiring the protein as a nucleation site. Solutions with higher polymer concentrations will tend to form larger particles as evidenced earlier for PGLA. Spraying a 5.0% *l*-PLA solution at 0.5 mL/min and 24 °C resulted in particles 250−500 μm in diameter, Figure 10 (bottom). This polymer precipitates very rapidly, and a polymer skin quickly forms on the droplet while still in the CO_2 vapor phase. The high solution viscosity caused the drop size to be larger than the nozzle inner diameter, and the resultant particle diameter was the same as the initial drop size. In this case the large polymer particles appeared to encapsulate all of the protein particles, as no individual protein particles were found on the sample slides.

Conclusions

Several major challenges for the PCA process were overcome in order to encapsulate a protein into PGLA. The PGLA particles were large enough to encapsulate the protein and did not agglomerate. In contrast, the primary particles (0.5 to 5 μm) were too small for encapsulation when the solution was sprayed into liquid or supercritical CO_2; furthermore, the particles were highly agglomerated. By delaying precipitation in a vapor CO_2 phase over a

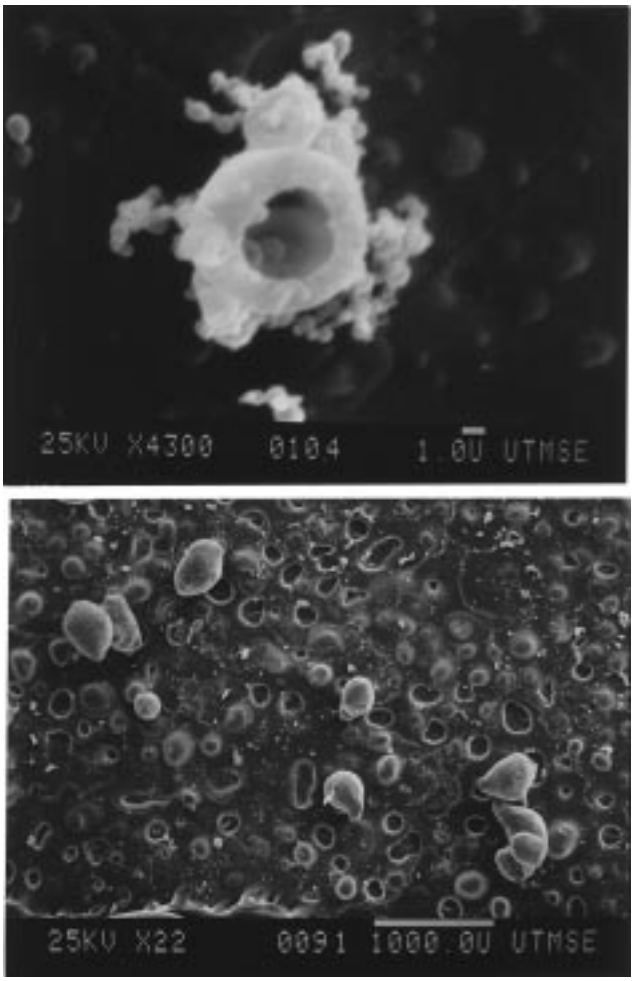

Figure 10—SEM micrographs of *l*-PLA microspheres formed by spraying a 1.0/0.1 wt % *l*-PLA/lysozyme suspension at 0.1 mL/min at 20 °C (top) and a 5.0/0.5 wt % *l*-PLA/lysozyme suspension at 0.5 mL/min at 24 °C (bottom) through a 100 μm capillary nozzle into static CO_2.

liquid CO_2 phase, much larger primary particles were formed, from 5 to 70 μm. At an optimal temperature of −20 °C, the polymer solution mixed rapidly with CO_2, and agglomeration of primary particles was minimal due to harder particles than at higher temperatures.

The amorphous polymer PGLA is highly plasticized by CO_2. Dissolution of CO_2 into PGLA depresses the T_g from the normal value of 45 °C to approximately −40 °C at 276 bar, based upon observation of particle agglomeration. Below −40 °C, the polymer remains as a nonsticky, free-flowing powder in the presence of CO_2 at 276 bar. Below −30 °C, the rate of mixing between CH_2Cl_2 and liquid CO_2 decreases appreciably. At an optimal temperature of −20 °C, the highly viscous PGLA microspheres do not agglomerate, yet the temperature is high enough to achieve adequate mixing between liquid CO_2 and the organic solution. An additional benefit of operating at colder temperatures is the relatively low pressure. At −20 °C, the saturation pressure of CO_2 is 19.7 bar, compared to 61.4 bar at 23 °C.

The vapor-over-liquid PCA process forms microspheres in the 5−70 μm range when a 5.0% solution of PGLA in dichloromethane is sprayed at 0.22 mL/min through a 100 μm diameter nozzle into static CO_2 at −20 °C. Experimental temperatures of 0 °C or above or below −30 °C yielded only large (>1000 μm) agglomerates. At high temperatures the particles are too sticky due to dissolved CO_2, and at low temperatures, the organic solution and CO_2 mix too slowly. Lower concentrations yielded smaller primary

particles whereas highly viscous concentrated solutions above 10.0 wt % led to skin formation in the vapor phase and subsequent agglomeration in the liquid CO_2 phase. The thin skin is weak due to low molecular weight and dissolved CO_2, and hence rupturing occurs upon impact at the liquid interface leading to agglomeration. Particle sizes did not change appreciably with solution flow rate in the "dripping" regime. At the onset of streaming flow, there was a higher percentage of large particles, while the particle size range remained the same. The most spherical and uniform particles ranging in size from 3 to 25 μm in diameter were produced by flowing CO_2 at high velocity through an annular region in a coaxial nozzle to provide mixing at the interface.

Encapsulation of 1−10 μm lysozyme particles proved successful for the 5−70 μm PGLA microspheres for a 1:10 ratio by weight of protein to polymer and a 5 wt % polymer solution. The presence of lysozyme in the particles was demonstrated by SEM analysis, optical microscopy, and EDS. A high encapsulation efficiency for this process is favored by the fact that the protein and polymer precipitate together in small droplets. The use of protein suspensions extends the applicability of the PCA process substantially, since many proteins are insoluble in organic solvents and are less likely to be denatured when suspended.

References and Notes

1. Mathiowitz, E.; Jacob, J. S.; Jong, Y. S.; Carino, G. P.; Chickering, D. E.; Chaturvedi, P.; Santos, C. A.; Vijayaraghavan, K.; Montgomery, S.; Bassett, M.; Morrell, C. Biologically Erodable Microspheres as Potential Oral Drug Delivery Systems. *Nature* **1997**, *386*, 410−4.
2. Cavalier, M.; Benoit, J. P.; Thies, C. The Formation and Characterization of Hydrocortisone-Loaded Poly((±)-Lactide) Microspheres. *J. Pharm. Pharmacol.* **1986**, *38*, 249−53.
3. Leelarasamee, N.; Howard, S. A.; Malanga, C. J.; Ma, J. K. H. A Method for the Preparation of Polylactic Acid Microcapsules of Controlled Particle Size and Drug Loading. *J. Microencapsulation* **1988**, *5*, 147−57.
4. Spenlehauer, G.; Veillard, M.; Benoit, J. P. Formation and Characterization of Cisplatin Loaded Poly(d,l-Lactide) Microspheres for Chemoembolization. *J. Pharm. Sci.* **1986**, *75*, 750−5.
5. Park, T. G.; Alonso, M. J.; Langer, R. Controlled Release of Proteins from Poly(L-Lactic acid) Coated Polyisobutylcyanoacrylate Microcapsules. *J. Appl. Polym. Sci.* **1994**, *52*, 1797−1807.
6. Thanoo, B. C.; Doll, W. J.; Mehta, R. C.; Digenis, G. A.; DeLuca, P. P. Biodegradable Indium-111 Labeled Microspheres for in Vivo Evaluation of Distribution and Elimination. *Pharm. Res.* **1995**, *12*, 2060−4.
7. Fong, J. W. Processes for Preparation of Microspheres; U.S. Patent 4384975, 1983.
8. Domb, A. J.; Amselem, S.; Maniar, M. Biodegradable Polymers as Drug Carrier Systems. In *Polymeric Biomaterials*; Dumitrius, S., Ed.; Marcel Dekker: New York, 1994; pp 399−433.
9. Puisieux, F.; Barratt, G.; Couarraze, G.; Couvreur, P.; Devissaguet, J. P.; Dubernet, C.; Fattal, E.; Fessi, H.; Vauthier, C.; Benita, S. Polymeric Micro- and Nanoparticles as Drug Carriers. In *Polymeric Biomaterials*; Dumitrius, S., Ed.; Marcel Dekker: New York, 1994; pp 749−94.
10. Langer, R. Polymeric Delivery Systems for Controlled Drug Release. *Chem. Eng. Commun.* **1980**, *6*, 1−48.
11. Lewis, D. H. Controlled Release of Bioactive Agents from Lactide/Glycolide Polymers. In *Biodegradable Polymers as Drug Delivery Systems*; M. Chasin, M., Langer, R., Eds.; Marcel Dekker: New York, 1990; Vol. 45, pp 1−41.
12. Alonso, M. J. Nanoparticulate Drug Carrier Technology. In *Microparticulate Systems for the Delivery of Proteins and Vaccines*; Cohen, S., Bernstein, H., Eds.; Marcel Dekker: New York, 1996; Vol. 77, pp 203−242.
13. Knutson, B. L.; Debenedetti, P. G.; Tom, J. W. Preparation of Microparticulates Using Supercritical Fluids. In *Microparticulate Systems for the Delivery of Proteins and Vaccines*; Cohen, S., Bernstein, H., Eds.; Marcel Dekker: New York, 1996; pp 89−125.
14. Johnston, K. P.; Kim, S.; Combes, J. Spectroscopic Determination of Solvent Strength and Structure in Supercritical Fluid Mixtures. *Am. Chem. Soc. Symp. Ser.* **1989**, *406*, 52−71.
15. McHugh, M. A.; Krukonis, V. J. *Supercritical Fluid Extraction Principles and Practice*, 2nd ed.; Butterworth: Stoneham, MA, 1994.
16. Matson, D. W.; Petersen, R. C.; Smith, R. D. Production of Powders and Films by the Rapid Expansion of Supercritical Solutions. *J. Mater. Sci.* **1987**, *22*, 1919−1928.
17. Matson, D. W.; Fulton, J. L.; Peterson, R. C.; Smith, R. D. Rapid Expansion of Supercritical Fluid Solutions: Solute Formation of Powders, Thin Films and Fibers. *Ind. Eng. Chem. Res.* **1987**, *26*, 2298−2306.
18. Tom, J. W.; Debenedetti, P. G. Formation of Bioerodible Microspheres and Microparticles by Rapid Expansion of Supercritical Solutions. *Biotechnol. Prog.* **1991**, *7*, 403−411.
19. Tom, J. W.; Debenedetti, P. G. Particle Formation with Supercritical Fluids − a Review. *J. Aerosol Sci.* **1991**, *22*, 555−584.
20. Phillips, E. M.; Stella, V. J. Rapid Expansion from Supercritical Solutions: Application to Pharmaceutical Processes. *Int. J. Pharm.* **1992**, 1−10.
21. Boen, S. N.; Bruch, M. D.; Lele, A. K.; Shine, A. D. Quick Quenching of Polymer Blends. In *Polymer Solutions, Blends, and Interfaces*; Noda, I., Rubingh, D. N., Eds.; Elsevier Science Publishers B. V.: Amsterdam, 1992; pp 151−172.
22. Lele, A. K.; Shine, A. D. Morphology of Polymers Precipitated From a Supercritical Solvent. *AICHE J.* **1992**, *38*, 742−752.
23. Lele, A. K.; Shine, A. D. Effect of RESS Dynamics on Polymer Morphology. *Ind. Eng. Chem. Res.* **1994**, *33*, 1476−1485.
24. Mawson, S.; Johnston, K. P.; Combes, J. R.; DeSimone, J. M. Formation of Poly(1,1,2,2-tetrahydroperfuorodecyl acrylate) Submicron Fibers and Particles from Supercritical Carbon Dioxide Solutions. *Macromolecules* **1995**, *28*, 3182−3191.
25. Alessi, P.; Cortesi, A.; Kikic, I.; Foster, N. R.; Macnaughton, S. J.; Colombo, I. Particle Production of Steroid Drugs Using Supercritical Fluid Processing. *Ind. Eng. Chem. Res.* **1996**, *35*, 4718−4726.
26. Kim, J. H.; Paxton, T. E.; Tomasko, D. L. Microencapsulation of Naproxen Using Rapid Expansion of Supercritical Solutions. *Biotechnol. Prog.* **1996**, *12*, 650−61.
27. Debenedetti, P. G.; Tom, J. W.; Yeo, S. D.; Lim, G. B. Application of Supercritical Fluids for the Production of Sustained Delivery Devices. *J. Controlled Release* **1993**, *24*, 27−44.
28. Gallagher, P. M.; Coffey, M. P.; Krukonis, V. J.; Klasuts, N. Gas Antisolvent Recrystallization: New Process To Recrystallize Compounds Insoluble in Supercritical Fluids. In *Supercritical Fluid Science and Technology*; K. P. Johnston, K. P., Penninger, J. M. L., Ed.; American Chemical Society: Washington, D. C., 1989; Vol. 406, pp 334−354.
29. Randolph, T. W.; Randolph, A. J.; Mebes, M.; Yeung, S. Sub-Micrometer-Sized Biodegradable Particles of Poly(L-Lactic Acid) via the Gas Antisovent Precipitation Process. *Biotechnol. Prog.* **1993**, *9*, 429−435.
30. Chou, Y. H.; Tomasko, D. L. GAS Crystallization of Polymer-Pharmaceutical Composite Particles. In *The 4th International Symposium on Supercritical Fluids*; International Society for the Advancement of Supercritical Fluids: Sendai, Japan, 1997; pp 55−7.
31. Dixon, D. J. Formation of Polymer Materials by Precipitation with a Compressed Fluid Antisolvent. Thesis, University of Texas at Austin, 1992.
32. Dixon, D. J.; Johnston, K. P.; Bodmeier, R. P. Polymeric Materials Formed by Precipitation with a Compressed Fluid Antisolvent. *AIChE J.* **1993**, *39*, 127−139.
33. Dixon, D. J.; Johnston, K. P. Formation of Microporous Polymer Fibers and Oriented Fibrils by Precipitation with a Compressed Fluid Antisolvent. *J. Appl. Polym. Sci.* **1993**, *50*, 1929−1942.
34. Dixon, D. J.; Luna-Barcenas, G.; Johnston, K. P. Microcellular Microspheres and Microballoons by Precipitation with a Vapour-Liquid Compressed Fluid Antisolvent. *Polymer* **1994**, *35*, 3998−4005.
35. Yeo, S. D.; Lim, G. B.; Debenedetti, P. G.; Bernstein, H. Formation of Microparticulate Protein Powders Using a Supercritical Fluid Antisolvent. *Biotechnol. Bioeng.* **1993**, *41*, 341−346.
36. Yeo, S.-D.; Debenedetti, P. G.; Radosz, M.; Schmidt, H.-W. Supercritical Antisolvent Process for Substituted Para-Linked Aromatic Polyamides: Phase Equilibrium and Morphology Study. *Macromolecules* **1993**, *26*, 6207−6210.
37. Luna-Barcenas, G.; Kanakia, S. K.; Sanchez, I. C.; Johnston, K. P. Semicrystalline Microfibrils and Hollow Fibres by Precipitation with a Compressed-Fluid Antisolvent. *Polymer* **1995**, *36*, 3173−3182.

38. Bodmeier, R. P.; Wang, H.; Dixon, D. J.; Mawson, S.; Johnston, K. P. Polymeric Microspheres Prepared by Spraying into Compressed Carbon Dioxide. *Pharm. Res.* **1995**, *12*, 1211−1217.
39. Mawson, S.; Johnston, K. P.; Betts, D. E.; McClain, J. B.; DeSimone, J. M. Stabilized Polymer Microparticles by Precipitation with a Compressed Fluid Antisolvent I. Polyfluoroacrylate Based Surfactants. *Macromolecules* **1997**, *30*, 71−77.
40. Mawson, S. The Formation and Characterization of Polymeric Materials Precipitated by CO_2-Based Spray Processes. Thesis, University of Texas at Austin, 1996.
41. Mawson, S.; Kanakia, S.; Johnston, K. P. Coaxial Nozzle for Control of Particle Morphology in Precipitation with a Compressed Fluid Antisolvent. *J. Appl. Polym. Sci.* **1997**, *64*, 2105−2118.
42. Mawson, S.; Kanakia, S.; Johnston, K. P. Metastable Polymer Blends by Precipitation with a Compressed Fluid Antisolvent. *Polymer* **1997**, *38*, 2957−2967.
43. Falk, R.; Randolph, T.; Meyer, J. D.; Kelly, R. M.; Manning, M. C. Controlled Release of Ionic Pharmaceuticals from Poly-(L-Lactide) Microspheres Produced by Precipitation with a Compressed Antisolvent. *J. Controlled Release* **1997**, *44*, 77−85.
44. Winters, M. A.; Knutson, B. L.; Debenedetti, P. B.; Sparks, H. G.; Przybycien, T. M.; Stevenson, C. L.; Prestrelski, S. J. Precipitation of Proteins in Supercritical Carbon Dioxide. *J. Pharm. Sci.* **1996**, *85*, 586−594.
45. Bleich, J.; Kleinebudde, P.; Müller, B. W. Influence of Gas Density and Pressure on Microparticles Produced with the ASES Process. *Int. J. Pharm.* **1994**, *106*, 77−84.
46. Bleich, J.; Müller, B. W. Production of Drug Loaded Microparicles by the Use of Supercritical Gases with the Aerosol Solvent Extraction System (ASES) Process. *J. Microencapsulation* **1996**, *13*, 131−9.
47. Fischer, W.; Müller, B. W. Method and Apparatus for the Manufacture of a Product Having a Substance Embedded in a Carrier; U.S. Patent 5043280, 1991.
48. McHugh, M. A.; Krukonis, V. Supercritical Fluids. In *Encyclopedia of Polymer Science and Engineering*, 2nd ed.; Mark, H. F., Bikales, N. M., Overberger, C. G., Menges, G., Eds.; John Wiley: New York, 1988; Vol. 16.
49. McHugh, M. A. Polymers in Supercritical Fluids. In *The 4th International Symposium on Supercritical Fluids*; International Society for the Advancement of Supercritical Fluids: Sendai, Japan, 1997; pp 785−8.
50. Ruchatz, F.; Kleinebudde, P.; Müller, B. W. Residual Solvents in Biodegradable Microparticles. Influence of Process Parameters on the Residual Solvent in Microparticles Produced by the Aerosol Solvent Extraction System (ASES) Process. *J. Pharm. Sci.* **1997**, *86*, 101−5.
51. Steckel, H.; Thies, J.; Müller, B. W. Micronizing of steroids for pulmonary delivery by supercritical carbon dioxide. *Int. J. Pharm.* **1997**, *152*, 99−110.
52. Falk, R. F.; Randolph, T. W. Process Variable Implications for Residual Solvent Removal and Polymer Morphology in the Formation of Gentamycin-Loaded Poly(L-lactide) Microparticles. *Pharm. Res.* **1998**, *15*, 1233−7.
53. Condo, P. D.; Paul, D. R.; Johnston, K. P. Glass Transitions of Polymers with Compressed Fluid Diluents: Type II and III Behavior. *Macromolecules* **1994**, *27*, 365−371.
54. Fong, J. W. *Processes for Preparation of Microspheres*; U.S. Patent 4166800, 1979.
55. Schwendeman, S. P.; Cardamone, M.; Klibanov, A.; Langer, R.; Brandon, M. R. Stability of Proteins and Their Delivery from Biodegradable Polymer Microspheres. In *Microparticulate Systems for the Delivery of Proteins and Vaccines*; Cohen, S., Bernstein, H., Eds.; Marcel Dekker: New York, 1996; Vol. 77, pp 1−49.
56. Yeo, S. D.; Debenedetti, P. G.; Patro, S. Y.; Przybycien, T. M. Secondary Structure Characterization of Microparticulate Insulin Powders. *J. Pharm. Sci.* **1994**, *83*, 1651−1656.
57. Winters, M. A.; Debenedetti, P. G.; Barey, J.; Sparks, H. G.; Sane, S. U.; Przybycien, T. M. Long-term and high-temperature storage of supercritically processed microparticulate protein powders. *Pharm. Res.* **1997**, *14*, 1370−8.
58. Kissel, T.; Koneberg, R. Injectable Biodegradable Microspheres for Vaccine Delivery. In *Microparticulate Systems for the Delivery of Proteins and Vaccines*; Cohen, S., Bernstein, H., Eds.; Marcel Dekker: New York, 1996; Vol. 77, pp 51−87.
59. Bleich, J.; Müller, B. W.; Wabmus, W. Aerosol solvent extraction system − a new microparticle production technique. *Int. Pharm.* **1993**, *97*, 111−7.
60. Lemert, R. M.; Fuller, R. A.; Johnston, K. P. Reverse Micelles in Supercritical Fluids. 3. Amino Acid Solubilization in Ethane and Propane. *J. Phys. Chem.* **1990**, *94*, 6021−28.
61. Bailey, P. D. *An Introduction To Peptide Chemistry*; John Wiley & Sons: New York, 1990; p 232.
62. Hamaguchi, K.; Hayashi, K. Lysozyme. In *Proteins: Structure and Function*; Funatsu, M., Hiromi, K., Imahori, K., Murachi, T., Narita, K., Eds.; John Wiley & Sons: New York, 1972; Vol. 1, pp 85−222.

Acknowledgments

We acknowledge support from NSF (CTS-9626828), DOE (DE-FG03-96ER14664), the Separations Research Program at the University of Texas at Austin, and the Texas Advanced Technology Program. We thank ISCO Corporation for the donation of the high-pressure syringe pump, and Alza for supplying the poly(DL-lactide-*co*-glycolide) and lysozyme samples.

JS980237H